

# LinearDesign: Efficient Algorithms for Optimized mRNA Sequence Design

He Zhang<sup>a,b</sup>, Liang Zhang<sup>b</sup>, Ziyu Li<sup>a</sup>, Kaibo Liu<sup>a</sup>, Boxiang Liu<sup>a</sup>, David H. Mathews<sup>c,d,e</sup>, and Liang Huang<sup>a,b,\*</sup>

<sup>a</sup>Baidu Research USA, Sunnyvale, CA 94089, USA; <sup>b</sup>School of Electrical Engineering & Computer Science, Oregon State University, Corvallis, OR 97330, USA; <sup>c</sup>Dept. of Biochemistry & Biophysics; <sup>d</sup>Center for RNA Biology; <sup>e</sup>Dept. of Biostatistics & Computational Biology, University of Rochester Medical Center, Rochester, NY 14642, USA

A messenger RNA (mRNA) vaccine has emerged as a promising direction to combat the current COVID-19 pandemic. This requires an mRNA sequence that is stable and highly productive in protein expression, features which have been shown to benefit from greater mRNA secondary structure folding stability and optimal codon usage. However, sequence design remains a hard problem due to the exponentially many synonymous mRNA sequences that encode the same protein. We show that this design problem can be reduced to a classical problem in formal language theory and computational linguistics that can be solved in  $O(n^3)$  time, where  $n$  is the mRNA sequence length. This algorithm could still be too slow for large  $n$  (e.g.,  $n = 3,822$  nucleotides for the spike protein of SARS-CoV-2), so we further developed a linear-time approximate version, LinearDesign, inspired by our recent work, LinearFold. This algorithm, LinearDesign, can compute the approximate minimum free energy mRNA sequence for this spike protein in just 16 minutes using beam size  $b = 1,000$ , with only 0.6% loss in free energy change compared to exact search (i.e.,  $b = +\infty$ , which costs 1.6 hours). We also develop two algorithms for incorporating the codon optimality into the design, one based on  $k$ -best parsing to find alternative sequences and one directly incorporating codon optimality into the dynamic programming. Our work provides efficient computational tools to speed up and improve mRNA vaccine development.

Availability: server: <http://rna.baidu.com/lineardesign>; code: to be released on GitHub.

## 1. Introduction

To defeat the current COVID-19 pandemic, which has already claimed 100,000+ deaths as of early April, a messenger RNA (mRNA) vaccine has emerged as a promising approach thanks to its rapid and scalable production and non-infectious and non-integrating properties. However, designing an mRNA sequence to achieve high stability and protein production remains a challenging problem. Recently, it is discovered that greater secondary structure folding stability and optimal codon usage synergize to increase protein expression.<sup>1</sup> The design problem can therefore be formulated as finding the mRNA sequence(s) that are good in both secondary structure stability and codon optimality among the exponentially many synonymous sequences that encode the same protein.

Each amino acid is translated by a codon, which is 3 adjacent mRNA nucleotides. For example, the start codon AUG translates into methionine, the first amino acid in any protein sequence. But due to redundancies in the genetic code ( $4^3 = 64$  triplet codons for 21 amino acids), most amino acids can be translated from multiple codons. This fact makes the search space of mRNA design increase exponentially with protein length, e.g., for the spike protein of SARS-CoV-2 (the virus that causes the COVID-19 pandemic), which contains 1,273 amino acids (plus the stop codon which is part of the mRNA but not part of a protein), there are about  $10^{632}$  mRNA candidates. The

mRNA design problem, therefore, aims to exploit the redundancies in the genetic code to find more stable and productive mRNA sequences than the wild type in nature.

Our key idea is to show that this design problem can be reduced to a classical problem in formal language theory and computational linguistics, namely the notion of intersection between a Stochastic Context Free Grammar (SCFG) and a Deterministic Finite Automaton (DFA). Here the SCFG represents the folding free energy model and the DFA represents the set of all possible synonymous mRNA sequences that code a given protein. While the use of SCFG in RNA folding is well-known,<sup>2</sup> the use of DFA to encode the mRNA search space and solving the design problem via the intersection of SCFG and DFA are novel. This intersection can be done in  $O(n^3)$  time, where  $n$  is the mRNA sequence length, but it could still be too slow for large  $n$  (e.g.,  $n = 3 \times (1273 + 1) = 3,822$  nucleotides for the spike protein of SARS-CoV-2), so we further developed a linear-time approximate version, LinearDesign, inspired by our recent work, LinearFold.<sup>3</sup> We also develop two algorithms for incorporating the codon optimality into the design, one based on  $k$ -best parsing to find alternative sequences and one directly incorporating codon optimality into the dynamic programming.

After the completion of our algorithm design and implementation of our Python prototype and C++ code, we became aware of two earlier, independent, papers that tackled the same problem of “most stable RNA design” using dynamic programming.<sup>4,5</sup> The second paper “CDSfold” published in 2016 did not cite the first one, published in 2003. Our work is different in three aspects. First, we reduced the mRNA design problem to “a context-free grammar intersecting a DFA”, a classical problem in formal language theory and computational linguistics, which is more general and can be applied to other scenarios with alternative inputs, whereas the previous algorithms were ad hoc. Second, we integrated codon optimality in the optimization. Third, we further developed a linear-time approximate version with greatly reduced runtime for long sequences and small sacrifices in search quality.

## 2. LinearDesign Algorithms

The mRNA design problem can be formulated as follows: given a protein sequence  $\mathbf{p} = p_1 \dots p_m$  where each  $p_i$  is an amino acid, we search, among all possible mRNA sequences  $\mathbf{r}$  that translate into protein  $\mathbf{p}$ , the best mRNA sequence  $\mathbf{r}^*(\mathbf{p})$ , defined as the sequence that has the structure with minimum folding free energy change:

$$\mathbf{r}^*(\mathbf{p}) = \underset{\mathbf{r} \in \text{RNA}(\mathbf{p})}{\text{argmin}} \text{MFE}(\mathbf{r}) \quad [1]$$

$$\text{MFE}(\mathbf{r}) = \min_{\mathbf{s} \in \text{structures}(\mathbf{r})} \Delta G^\circ(\mathbf{r}, \mathbf{s}) \quad [2]$$

The authors declare no conflict of interest.

\*Corresponding author: liang.huang.sh@gmail.com.

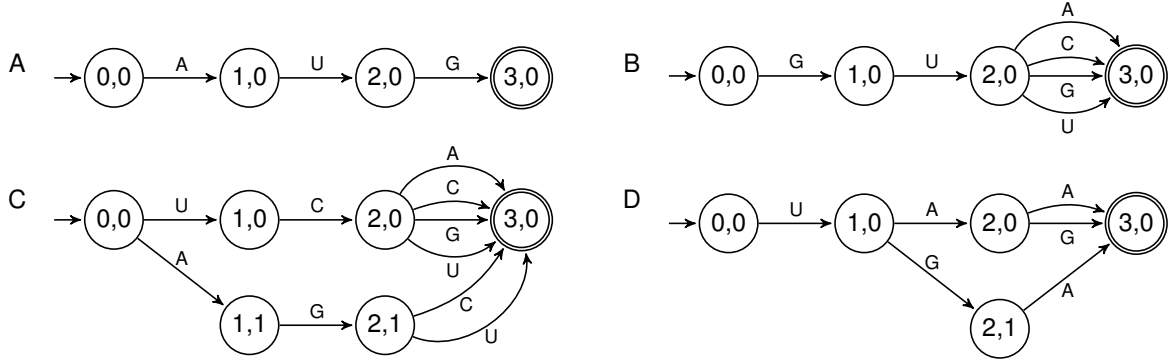


**Fig. 1.** Four examples of Deterministic Finite Automaton (DFA) representations for amino acids. Each example represents one amino acid. **A:** DFA for methionine, with only one path (tryptophan is the only other amino acid with a single codon path in the standard genetic code); **B:** DFA for valine, with alternatives only at the third nucleotide (15 of 21 amino acids are like this, with 2–4 paths); **C:** DFA for serine, which branches at the start node and has a total of 6 paths (leucine and arginine are also like this); **D:** DFA for the stop codon.

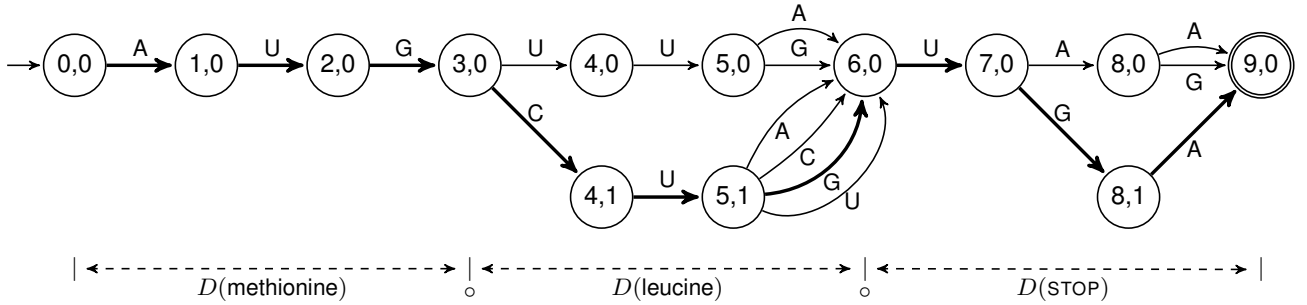


**Fig. 2.** The protein DFA for “methionine leucine” by concatenating small DFAs from individual amino acids, i.e.,  $D(\text{methionine}) \circ D(\text{leucine}) \circ D(\text{STOP})$ . The thick arrows indicate the best mRNA sequence after intersecting this DFA with the context-free grammar (see Fig. 3).

where  $\text{RNA}(\mathbf{p}) = \{\mathbf{r} \mid \text{protein}(\mathbf{r}) = \mathbf{p}\}$  is the search space,  $\text{structures}(\mathbf{r})$  is the set of all possible secondary structure for RNA sequence  $\mathbf{r}$ , and  $\Delta G^\circ(\mathbf{r}, \mathbf{s})$  is the free energy change of structure  $\mathbf{s}$  for RNA  $\mathbf{r}$  according to an energy model. Note that the mRNA sequence length is  $n = 3(m + 1)$  due to the final stop codon, which is not translated into the protein sequence.

Next we first show how to represent the exponentially large search space  $\text{RNA}(\mathbf{p})$  compactly via DFAs, and then discuss how to do this **argmin** search (over the product of two exponentially large spaces) efficiently via dynamic programming, which can be reduced to the CFG intersection with DFA.

**A. DFA representation for amino acid codons and mRNA search space.** In the fields of formal language theory and computational linguistics, the DFA graph is typically used to encode ambiguities in languages.<sup>6</sup> We notice that the ambiguity of codon choice for amino acid is similar as to the language ambiguity problem, and can be represented with a DFA graph too. We first illustrate how to represent the amino acid codons using DFAs.

Informally, a DFA is a directed graph with labeled edges and distinct start and end nodes. For our purpose each edge is labeled by a nucleotide, so that each start-to-end path represents a triplet codon. Formally, a DFA is a 5-tuple  $\langle Q, \Sigma, \delta, q_0, F \rangle$  where  $Q$  is the set of nodes,  $\Sigma$  is the alphabet (here  $\Sigma = \{A, C, G, U\}$ ),  $q_0$  is the start node,  $F$  is the set of end nodes (in this work the end node is unique, i.e.,  $|F| = 1$ ), and  $\delta$  is the transition function that takes a node  $q$  and a symbol  $a \in \Sigma$  and returns the next node  $q'$ , i.e.,  $\delta(q, a) = q'$  encodes a labeled edge  $q \xrightarrow{a} q'$ .

Fig. 1 illustrates how DFAs represent 4 different types of amino acids and their codons. All these DFAs have  $(0, 0)$  and  $(3, 0)$  as their start and end nodes, respectively. Fig. 1A is the DFA representation for methionine, which has only one path. Fig. 1B is the DFA for amino acid valine, whose codon has a choice at the third nucleotide (most amino acids are of this type). Fig. 1C represents the most complex case, serine, leucine, and arginine, which have 6 codons each, and the branching happens at the start node. Fig. 1D is the DFA for the stop codon. It is special because branching happens at the second step, at node  $(1, 0)$ .

After building DFAs for each amino acid, we can concatenate them into a single DFA  $D(\mathbf{p})$  for a protein sequence  $\mathbf{p}$ , which represents all possible mRNA sequences that translate into that protein

$$D(\mathbf{p}) = D(p_1) \circ D(p_2) \circ \dots \circ D(p_m) \circ D(\text{STOP})$$

by stitching the end node of each DFA with the start node of the next. The new end node of the protein DFA is  $(3(m + 1), 0)$ . Fig. 2 gives a DFA of the protein sequence “methionine leucine”.

We also define  $\text{out\_edges}(q)$  to be set of outgoing edges from node  $q$ , and  $\text{in\_edges}(q)$  to be the set of incoming edges:

$$\begin{aligned} \text{out\_edges}(q) &= \{(q', a) \mid \delta(q, a) = q'\} \\ \text{in\_edges}(q) &= \{(q', a) \mid \delta(q', a) = q\} \end{aligned}$$

For the DFA in Fig. 2,  $\text{out\_edges}((3, 0)) = \{((4, 0), U), ((4, 1), C)\}$  and  $\text{in\_edges}((9, 0)) = \{((8, 0), A), ((8, 0), G), ((8, 1), A)\}$ .

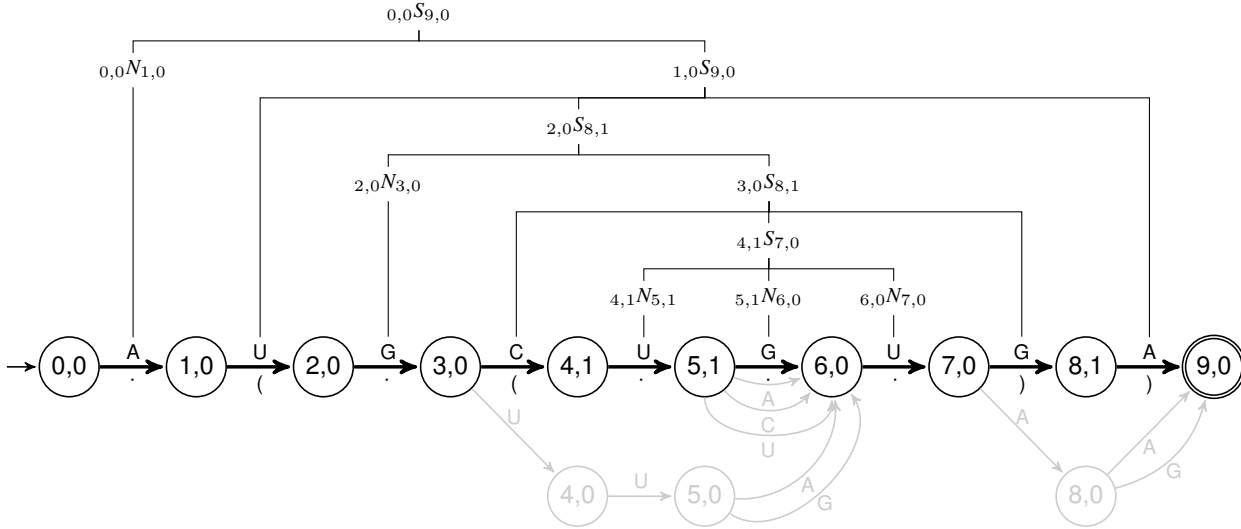


**Fig. 3.** One of the best derivations of the intersected grammar, demonstrating the path through the SCFG and the DFA (there are multiple best trees due to the simple energy model). The corresponding secondary structure (in dot-bracket format) is shown below the solid arrows. The rest of the DFA (from Fig. 2) is shown in light gray.

**B. CFG intersection with DFA.** A stochastic context-free grammar (SCFG) is a context-free grammar in which each rule is augmented with a weight. More formally, an SCFG is a 4-tuple  $(N, \Sigma, P, S)$  where  $N$  is the set of non-terminals,  $\Sigma$  is the set of terminals (identical to the alphabet in the DFA, in this case  $\{A, C, G, U\}$ ),  $P$  is the set of weight-associated context-free writing rules, and  $S \in N$  is the start symbol. Each rule in  $P$  has the form  $A \xrightarrow{w} (N \cup \Sigma)^*$  where  $A \in N$  is a non-terminal that can be rewritten according to this rule into a sequence of non-terminals and terminals (\* means repeating zero or more times) and  $w \in \mathbb{R}$  is the weight associated with this rule.

SCFGs are used to represent RNA folding. The weight of a derivation (parse tree, or a secondary structure in this case) is the sum of weights of the productions used in that derivation.<sup>2</sup>

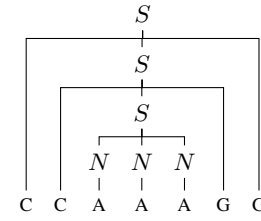
For example, for the very simple Nussinov-Jacobson model<sup>7</sup> (which simplifies the energy model to the number of base pairs), we can define this SCFG  $G$ :

$$\begin{aligned}
S &\xrightarrow{0} S S \\
S &\xrightarrow{-1} A S U \mid U S A \mid C S G \mid G S C \mid G S U \mid U S G \\
S &\xrightarrow{0} N S \mid S N \mid N N N \\
N &\xrightarrow{0} A \mid C \mid G \mid U
\end{aligned}$$

Here the first line is the bifurcating case, the second line is the base-pairing case (with weight  $-1$ , and the negative score mirrors the free energy minimization problem), and the third line is the unpaired cases (note  $S \xrightarrow{0} N N N$  makes sure the minimum hairpin length is 3, i.e., no sharp turn is allowed).

The standard RNA secondary structure prediction problem under a Nussinov model can be cast a parsing problem: given the above SCFG  $G$  and an input RNA sequence, what is the minimum-weight derivation in  $G$  that can generate sequence?

For example, for input CCAAAGG, the best derivation is



The mRNA design problem is now a simple extension of the above single-sequence folding problem to the case of multiple inputs: instead of finding the minimum energy structure (minimum weight derivation) for a given sequence, we find the minimum energy structure (and its corresponding sequence) among all possible structures for all possible sequences. This can be solved by intersecting the SCFG  $G$  on the protein DFA  $D$ , which results in a bigger SCFG

$$G' = G \cap D$$

and find the best derivation in  $G'$ .<sup>6</sup>

In the intersected grammar  $G'$ , each nonterminal has the form  $q_1 A q_2$ , where  $A \in N$  is an original nonterminal in  $G$  and  $q_1$  and  $q_2$  are two nodes in  $D$ ; and the new start symbol is  $q_0 S q_n$  where  $S$  is the original start symbol in  $G$  and  $q_0$  and  $q_n$  are the start and end nodes in  $D$ . The bifurcation rule  $S \xrightarrow{0} S S$  will become

$$q_1 S q_3 \xrightarrow{0} q_1 S q_2 q_2 S q_3$$

for all  $(q_1, q_2, q_3)$  node triplets in  $D$ . We can see that this is a generalization of the CKY algorithm<sup>8</sup> where  $(q_1, q_2, q_3)$  would be three string indices  $(i, k, j)$ . The terminal rule  $N \xrightarrow{0} A$  will become

$$q_1 N q_2 \xrightarrow{0} q_1 A q_2$$

if only if there is a labeled edge  $q_1 \xrightarrow{A} q_2$  in  $D$ , i.e.,  $\delta(q_1, A) = q_2$ .

This intersected grammar  $G'$  will have  $N|Q|^2$  nonterminals and  $P|Q|^3$  rules in the worst case ( $|Q|$  is the number of nodes in  $D$ ). This resembles the space and time complexities of the CKY algorithm (where  $|Q| = n$ ). Indeed, intersection is a generalization of CKY from fixed input (RNA folding) to lattice input (mRNA design).

```

1: function BOTTOMUPDESIGN( $\mathbf{p}$ )
2:  $n \leftarrow 3 \cdot |\mathbf{p}| + 1$   $\triangleright$  mRNA length; +1 for the stop codon
3:  $D \leftarrow D(x_1) \circ D(x_2) \circ \dots \circ D(\text{stop})$   $\triangleright$  build protein DFA
4:  $best \leftarrow \text{hash}()$   $\triangleright$  hash table: from  $[q_i, q_j]$  to score
5:  $back \leftarrow \text{hash}()$   $\triangleright$  hash table: from  $[q_i, q_j]$  to backpointer
6: for  $i = 0 \dots (n - 1)$  do
7:   for each  $q_i \in \text{nodes}(D, i)$  do
8:     for each  $(q_{i+1}, nuc_i) \in \text{out\_edges}(D, q_i)$  do
9:        $best[q_i, q_{i+1}] \leftarrow 0$   $\triangleright$  singleton:  $N \xrightarrow{0} A | C | G | U$ 
10:       $back[q_i, q_{i+1}] \leftarrow nuc_i$ 
11:  for  $l = 2 \dots n$  do
12:    for  $i = 0 \dots (n - l)$  do
13:       $j \leftarrow i + l$ 
14:      for each  $q_i \in \text{nodes}(D, i)$  do
15:        for each  $q_j \in \text{nodes}(D, j)$  do
16:          if  $j - i > 4$  then  $\triangleright$  pairing (no sharp turn)
17:            for each  $(q_{i+1}, nuc_i) \in \text{out\_edges}(D, q_i)$  do
18:              for each  $(q_{j-1}, nuc_{j-1}) \in \text{in\_edges}(D, q_j)$  do
19:                if  $\text{match}(nuc_i, nuc_{j-1})$  then
20:                   $score \leftarrow best[q_{i+1}, q_{j-1}] - 1$   $\triangleright S \xrightarrow{-1} A S U | \dots$ 
21:                   $\text{UPDATE}(q_i, q_j, score, (nuc_i, q_{i+1}, q_{j-1}, nuc_{j-1}))$ 
22:                for  $k = (i + 1) \dots (j - 1)$  do  $\triangleright$  bifurcation
23:                  for each  $q_k \in \text{nodes}(D, k)$  do
24:                     $score \leftarrow best[q_i, q_k] + best[q_k, q_j]$   $\triangleright S \xrightarrow{0} S S$ 
25:                     $\text{UPDATE}(q_i, q_j, score, q_k)$ 
26:  return  $best[q_0, q_n], \text{BACKTRACE}(q_0, q_n)$ 

```

**Fig. 4.** The pseudocode of a simplified bottom-up version of the mRNA Design algorithm. See Fig. SI 1 for UPDATE and BACKTRACE functions.

Now we just need to find the best (minimum weight) derivation in  $G'$ , from which we can read off the best mRNA sequence and its corresponding structure. Fig. 3 shows one of the best derivations for the DFA in Fig. 2.

**C. Bottom-up dynamic programming on Nussinov model.** We describe how to do dynamic programming based on CFG intersection with DFA. First, we use bottom-up dynamic programming on the Nussinov-Jacobson energy model as an introduction.

Fig. 4 gives the pseudocode for this simplified version. We first build up the given protein's DFA graph, and initialize two hash tables,  $best$  to store the best score for each state, and  $back$  to store the best backpointer for each state. The base cases (singleton rule) are  $best[q_i, q_{i+1}] \leftarrow 0$  and  $back[q_i, q_{i+1}] \leftarrow nuc_i$  for each state  $(q_i, q_{i+1})$ , where  $nuc_i$  is the edge between  $q_i$  and  $q_{i+1}$ . Next, for each state  $(q_i, q_j)$  it goes through the pairing rule and bifurcation rules, and updates if a better score is found. After filling out the hash tables bottom-up, we can backtrace the best mRNA sequence stored with the backpointers. See Fig. SI 1 for details of Update and Backtrace functions.

**D. Left-to-right dynamic programming with beam pruning.** The algorithm based on bottom-up dynamic programming runs in cubic time, however, it is still slow for long sequences. Inspired by our previous work, LinearFold,<sup>3</sup> we further developed a linear-time approximation algorithm for mRNA design. We apply beam pruning,<sup>9</sup>

```

1: function LINEARDESIGN( $\mathbf{p}, b$ )  $\triangleright b$  is beam size
2: for  $j = 1 \dots n$  do
3:   for each  $q_{j-1} \in \text{nodes}(D, j - 1)$  do
4:     for each  $q_i$  such that  $[q_i, q_{j-1}] \in best$  do
5:       for each  $(q_j, nuc_{j-1}) \in \text{out\_edges}(D, q_{j-1})$  do
6:          $backpointer \leftarrow (q_{j-1}, nuc_{j-1})$ 
7:          $\text{UPDATE}(q_i, q_j, best[q_i, q_{j-1}], backpointer) \triangleright S \xrightarrow{0} S N$ 
8:       if  $j - (i - 1) > 4$  then
9:         for each  $(q_{i-1}, nuc_{i-1}) \in \text{in\_edges}(D, q_i)$  do
10:          if  $\text{match}(nuc_{i-1}, nuc_{j-1})$  then  $\triangleright S \xrightarrow{-1} S A S U | \dots$ 
11:            for each  $q_k$  such that  $[q_k, q_{i-1}] \in best$  do
12:               $score \leftarrow best[q_k, q_{i-1}] + best[q_i, q_{j-1}] - 1$ 
13:               $backpointer \leftarrow (q_{i-1}, nuc_{i-1}, q_i, q_{j-1}, nuc_{j-1})$ 
14:               $\text{UPDATE}(q_k, q_j, score, backpointer)$ 
15:             $\text{BEAMPRUNE}(best, j, b) \triangleright$  choose top- $b$  among all  $(q_i, q_j)$ 's
16:  return  $best[q_0, q_n], \text{BACKTRACE2}(q_0, q_n)$ 

```

**Fig. 5.** The pseudocode of (simplified) LinearDesign algorithm. The first 10 lines are the same as in BOTTOMUPDESIGN (see Fig. 4). See Fig. SI 1 for UPDATE, BACKTRACE2, and BEAMPRUNE functions.

a classical pruning technique, to significantly narrow down the search space without sacrificing too much search quality.

Fig. 5 gives the pseudocode of simplified LinearDesign algorithm for the Nussinov model, based on left-to-right dynamic programming and beam pruning. LinearDesign replaces bottom-up dynamic programming with a left-to-right parsing. At each step  $j$  (the  $j$ th position of mRNA sequence), we only keep the top  $b$  states with the lowest free energy and prune out the less promising states, since they are unlikely to be the optimal sequence. Here  $b$ , the beam size, is a user-adjustable parameter to balance runtime and search quality. This approximation leads to a significant runtime reduce from  $O(n^3)$  to  $O(nb^2)$ . Notice that we use  $b = 100$  as default in LinearFold,<sup>3</sup> but in LinearDesign we usually use a larger  $b$  because the search space is much larger.

**E. Implementation on Turner model.** Our real system uses a left-to-right dynamic programming with beam pruning on the Turner nearest neighbor free energy model.<sup>10,11</sup> We implement the thermodynamic parameters following Vienna RNAfold,<sup>12</sup> except for the dangling ends and special hairpins. Dangling ends refer to stabilizing interactions for multiloops and external loops, which require knowledge of the nucleotide sequence outside of the state  $(q_i, q_j)$ . Though it could be integrated in LinearDesign, the implementation becomes more involved. Special hairpins are hairpin loop sequences of length 3, 4, or 6 unpaired nucleotides with folding free energies stored in lookup tables, rather than estimated from features like other sequences. Special hairpins can be also integrated in LinearDesign with some preprocessing. We will include both dangling end and special hairpin stabilities in future versions.

**F. MFE and CAI joint optimization.** Since CAI is also important for mRNA functional half life,<sup>1</sup> we consider optimizing MFE and CAI jointly. We add CAI as an additive regularization term in the

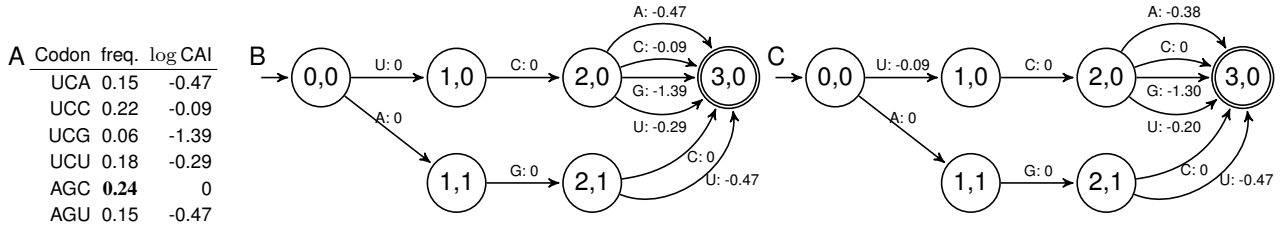


**Fig. 6.** The DFA representation integrating CAI as edge weight. **A:** Codon table of "serine". **B:** DFA graph of "serine" with CAI as edge weight; weights only differ at the last edges. **C:** Improved edge weights to differ earlier.

objective function:

$$\begin{aligned}
 \mathbf{r}^*(\mathbf{p}) &= \underset{\mathbf{r} \in \text{RNA}(\mathbf{p})}{\text{argmin}} \left( \text{MFE}(\mathbf{r}) - (m+1)\lambda \log \text{CAI}(\mathbf{r}) \right) \\
 &= \underset{\mathbf{r} \in \text{RNA}(\mathbf{p})}{\text{argmin}} \left( \text{MFE}(\mathbf{r}) - (m+1)\lambda \log \left( \prod_{i=1}^{m+1} w_i(\mathbf{r}) \right)^{\frac{1}{m+1}} \right) \\
 &= \underset{\mathbf{r} \in \text{RNA}(\mathbf{p})}{\text{argmin}} \left( \text{MFE}(\mathbf{r}) - \lambda \sum_{i=1}^{m+1} \log w_i(\mathbf{r}) \right)
 \end{aligned}$$

where  $m$  is the protein length,  $\log w_i(\mathbf{r})$  is the measurement of deviation from the optimal codon (0 is optimal) for the  $i$ th amino acid (given an mRNA candidate), and  $\lambda$  is a hyperparameter that balances MFE and CAI.

We integrate this equation into LinearDesign dynamic process, i.e., each DFA graph's edge will have a cost so that the combined cost of traversing a local path (choosing a codon) equals  $\log w_i$ . Each edge cost is the "best" of the paths (i.e., codons) that uses this edge.

Fig. 6 uses serine as an example, showing how to integrating CAI as edge cost in DFA graph. The 6 codons of serine, listed in Fig. 6A with their CAI, each has a corresponding path in the DFA graph (see Fig. 6B). For example, codon UCU has a CAI of 0.18, while the best codon AGC has a CAI of 0.24. The edge costs in "UCU path" are 0, 0,  $\log(0.18/0.24) = -0.29$ , therefore,  $\log w_i$  of UCU is -0.29. The best codon AGC has a  $\log w_i$  of 0, meaning that choosing AGC would not have a cost.

Considering LinearDesign is doing left-to-right dynamic programming with beam pruning, and at each step  $j$  states with lower scores are pruned, it is better to incur edge costs as early as possible in a path, which ensures the states with better CAI paths are more likely to survive in each step. Fig. 6C rearranges the edge cost to fit better for LinearDesign. Note that different edge costs in Fig. 6B and C would not affect exact search.

**G. The top  $k$  best mRNA candidates.** An alternative solution for finding mRNA candidates with both stable secondary structure and high CAI is to provide the top  $k$  mRNA candidates with the lowest MFE, and post-process them by features such as CAI. Although this is not as principled as the algorithm described in subsection 2F, this solution is easier to implement, and is more flexible in the sense that users are free to add other customized filters.

Inspired by the  $k$ -best parsing algorithm,<sup>13</sup> we developed an efficient algorithm to find suboptimal candidates in a sorted order. During the dynamic programming process (forward-phase), instead of just saving the single best prestate as the backpointer for each state, we store alternative prestates that all transit to this state. Then in the backtrace process (backward-phase), starting from the last state, we query the second best. The answer is one of the two cases: (1) the second best is from another prestate  $S_1$ ; or (2) the second best is from the same prestate  $S_0$ . In the former case we can find the second best

by backtracing the best path going through prestate  $S_1$ , while in the latter case we keep querying for the second best from the prestate  $S_0$ . Recursively, we would compute and get as many solutions as needed.

To our knowledge, our algorithm is the first one to output suboptimal results in the mRNA design problem. Two previous algorithms explored searching suboptimal secondary structure for RNA folding problem.<sup>14,15,16</sup> Zuker's algorithm is to find diverse suboptimal secondary structures in a given free energy gap. Our algorithm is different from these two in the sense that: (1) ours is for mRNA design problem; and (2) ours can output all top  $k$  best candidates in a sorted order.

Combining the  $k$ -best algorithm and linearization, LinearDesign is able to quickly design a large set of mRNA candidates, which provide a set of alternative designs for follow up with wet lab experiments.

### 3. Results

**A. Efficiency and scalability.** To estimate the run-time complexity of LinearDesign, we use 100 protein sequences from Uniprot<sup>17</sup> following CDSfold, with length from 78 to 2,828 *nt* (not including the stop codon). We found that there are three sequences whose lengths reported in CDSfold do not match the ones currently in Uniprot, so we removed these sequences, resulting in a dataset with 97 diverse protein sequences.

We compared LinearDesign in exact (infinite beam size) and approximate modes (beam size  $b = 1,000$  and  $b = 100$ ). Because CDSfold code is not currently available, we directly use the runtime reported in CDSfold paper as a comparison allowing us to compare the computational complexity. Note that CDSfold results and our results were run in different machines. We run LinearDesign on a machine with 2 Intel Xeon E5-2660 v3 CPUs (2.60 GHz), while CDSfold is run on the Chimera cluster system at AIST, which was reported in the paper as 176 Intel Xeon E5550 CPUs (2.53 GHz). Fig. 7 shows the runtime plots. We can see that CDSfold has an estimated runtime complexity of  $O(n^{3.1})$ , while LinearDesign (exact mode  $b = \infty$ ) runs in a complexity of  $O(n^{2.8})$ . Both CDSfold and LinearDesign ( $b = \infty$ ) have nearly cubic runtime, but LinearDesign ( $b = \infty$ ) is under the exact  $O(n^3)$  because we use the "jump" trick as in LinearFold,<sup>3</sup> i.e., jump to the next possible nucleotide  $nuc_j$  that can pair with  $nuc_i$  (with the help of preprocessing), instead of checking all positions one by one. In terms of the time cost, CDSfold takes 31 hours for the longest sequence in the dataset (8,484 *nt*), while LinearDesign ( $b = \infty$ ) takes 17 hours. If applying beam pruning, the runtime of LinearDesign reduces to linear complexity as expected. With beam size  $b = 1,000$ , the runtime is  $O(n^{1.2})$ , and further reduces to  $O(n^{1.0})$  with  $b = 100$ . Our LinearDesign finishes the longest sequence design in 46 minutes with  $b = 1,000$ , and in only 3 minutes with  $b = 100$ , which is 340 $\times$  speed up compared with the LinearDesign exact search.

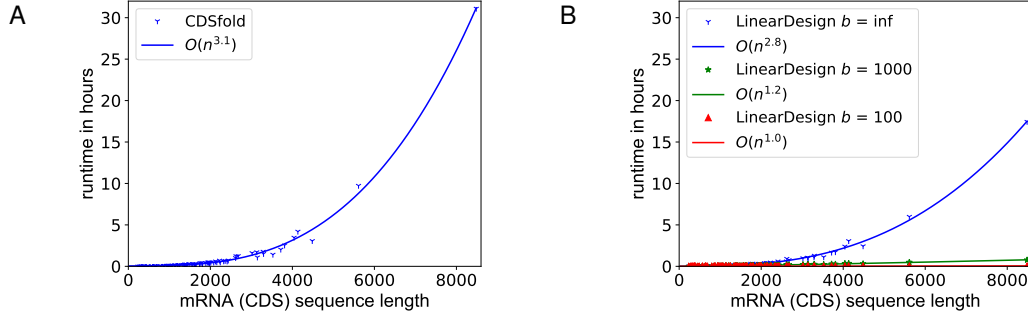


**Fig. 7.** Runtime comparison between CDSfold and LinearDesign on Uniprot dataset. **A:** the runtime of CDSfold as reported by Terai et al. **B:** the runtime of LinearDesign (exact mode  $b = \infty$ , and approximation mode  $b = 1,000$  and  $b = 100$ ) run by us on an Intel Xeon E5-2660 v3 CPU.

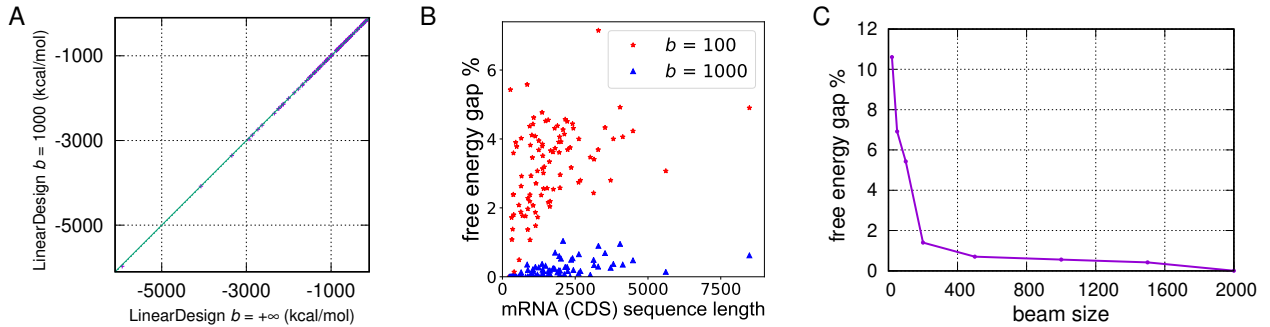


**Fig. 8.** Search quality of LinearDesign with beam pruning is good. **A:** LinearDesign with  $b = 1,000$  has small free energy gap compared with exact search. **B:** LinearDesign free energy gap percentage changes linearly with mRNA sequence length for both  $b = 100$  and  $b = 1,000$  on Uniprot dataset. **C:** LinearDesign free energy gap percentage changes with beam size for the spike protein of SARS-CoV-2.

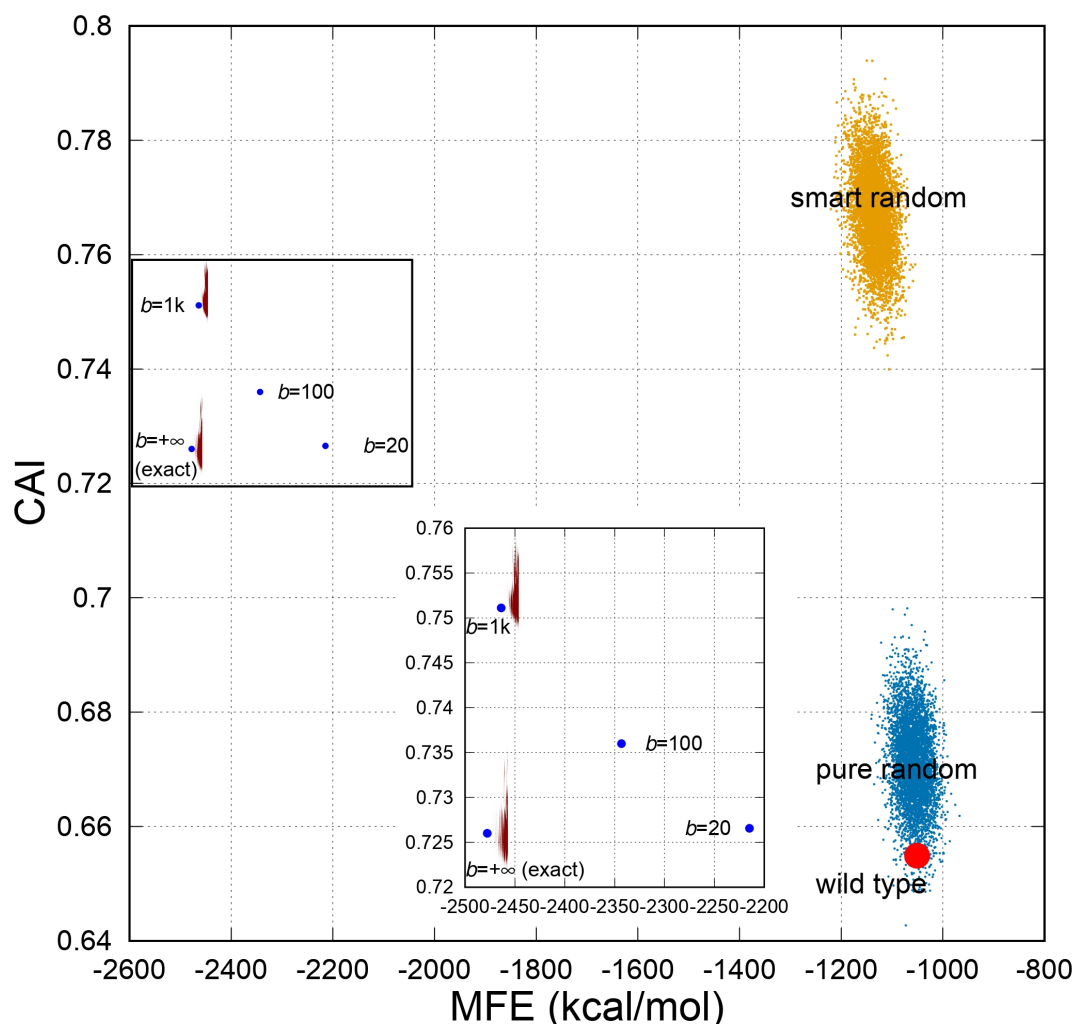
**B. Search quality of linear-time approximation.** Since the LinearDesign algorithm is significantly faster than its exact counterpart, we envision that the LinearDesign algorithm will be used for long sequences. To ensure the quality of the approximation used in LinearDesign (with beam pruning mode), we compared the energy gap between the exact ( $b = \infty$ ) and approximate algorithm ( $b = 1,000$ ). For this analysis, we used the same dataset as in subsection 3A.

Fig. 8 represents the free energy changes between the exact search and approximation. Fig. 8A compares free energy changes of the mRNA sequences designed with exact search and with  $b = 1,000$  approximation. The x-axis is the free energy of exact search, while the y-axis is the free energy of approximation. We see that all plots are on or close to the diagonal, which confirms that the free energy differences are 0 or small. Fig. 8B shows the trend of free energy changes increase linearly with mRNA sequence length. The y-axis is the percentage of free energy change gap, which is the free energy change gap ( $\Delta\Delta G^\circ$ ) divided by the free energy change of the MFE structure ( $\Delta G^\circ$ ). The percentage of free energy change gap is small for all sequences in the dataset. For  $b = 1,000$ , all sequences have gaps within 1%. Even for the longest sequence (8,484 nt), the gap is 0.8%. For  $b = 100$ , most gaps are within 5%, and the largest gap is 7%. We also investigate the percentage of free energy change gap against beam size for the spike protein of SARS-CoV-2 in Fig. 8C. Starting with a small beam size  $b = 20$ , the gap is 10.6%. With increasing beam size, the gap shrinks quickly to less than 6% at  $b = 100$ . Further increasing  $b$  up to 500, the gap drops to 1%. With a beam size of  $b = 2,000$  the gap drops to 0, which indicates that the approximation result is the same as exact search.

**C. Example for the coding mRNA of the spike protein.** The spike protein of SARS-CoV-2, which has 1,273 amino acid residues, is the target of mRNA vaccines (<https://clinicaltrials.gov/ct2/show/NCT04283461>). Therefore, we use the spike protein of SARS-CoV-2 as an example, and compare our designed sequences with the wildtype sequence and random generated sequences.

We use the mRNA sequence from the reference genome of SARS-CoV-2 (<https://www.ncbi.nlm.nih.gov/nuccore/MN908947>) as the wildtype sequence, which contains 3,822 nucleotides (including the stop codon). Additionally, we use two different strategies to generate random sequences (5,000 sequences for each strategy) as another baseline. One of the two strategies, named "pure random", is to randomly (with equal probabilities) choose a codon for each amino acid in the spike protein, and form a mRNA sequence by concatenation. The other strategy, called "smart random", is to choose a codon with the probabilities proportion to its usage frequency. We also run LinearDesign (in both exact mode and approximation mode) to evaluate the best sequences we can achieve. Since previous studies show that both mRNA secondary structure folding free energy change and codon optimality influence the stability and expression level in the host organism,<sup>1</sup> we do a two-dimensional comparison, MFE and codon adaptation index (CAI),<sup>18</sup> between mRNA sequences.

Fig. 9 shows the results. The wildtype sequence, denoted in a red circle, folds into a structure with the minimum free energy change of -1075.40 kcal/mol, and has a low CAI of 0.655. Most "pure random" sequences, denoted in blue plots, have similar free energy changes (-1057.77 kcal/mol on average) as the wildtype, but with higher CAI (0.671 on average). This may be because SARS-CoV-2 just recently



**Fig. 9.** Two-dimensional comparisons (MFE and CAI) between wildtype mRNA sequence (light red circle), random sequences (blue dots for pure random and orange dots for smart random) and our designed mRNA sequences (blue and dark red spots) on the spike protein of SARS-CoV-2. Our design includes the optimal mRNA sequence (with lowest MFE) in exact mode and approximation mode ( $b = 1,000$ ,  $b = 100$  and  $b = 20$ , respectively). The inset graph shows the plots of our designed  $k$  best sequences (top 10,000,000 plots for exact mode and top 2,000,000 for  $b = 1,000$ ).

infected human cells and does not have enough mutations to optimize for human codons. Compared with the wildtype and "pure random" sequences, "smart random" sequences, denoted in orange plots, have much higher CAI (0.768 on average), and slight improvement on MFE (-1134.59 kcal/mol on average). We also notice that both "pure random" and "smart random" sequences are packed in cloud-shaped small regions. This is because the search space of possible mRNAs is extremely huge and most of the random sequences have similar MFE and CAI. On the left (with much lower MFE) we plot our designed sequences. The leftmost one is the sequence designed in exact search mode, which has the lowest MFE of -2,477.70 kcal/mol and a CAI of 0.726. The MFE gap between our best designed sequence and the wildtype, as well as random sequences, is large (more than 1200 kcal/mol). With only 0.62% MFE loss from the exact search sequence, the designed sequence with beam size  $b = 1,000$  achieves a higher CAI of 0.751. For  $b = 100$  and  $b = 20$ , the MFE are still lower than -2,100 kcal/mol, with CAI both at around 0.735 and 0.725, respectively. Our designed sequences, for both exact search sequence

and approximate search sequences, are much better than random ones and the wildtype in terms of MFE and CAI.

We also show the top 10,000,000 best sequences for exact mode and top 2,000,000 for  $b = 1,000$ , and enlarge them in the inset graph in Figure 9. The MFE of the sequences are very close to the optimal one, and the free energy gap are within 20 kcal/mol. Some of the sequences have higher CAI, e.g., some of sequences have CAI higher than 0.730 in exact mode (bottom-left dark red cloud), and some of sequences have CAI higher than 0.755 for  $b = 1,000$  (top-left dark red cloud) This shows that our  $k$  best algorithm can be used to select sequences with much lower MFE and relative higher CAI as vaccine candidates.

Figure 10 shows the secondary structures of the wildtype mRNA sequences the best "smart random" sequence, and our designed sequence with lowest MFE (exact mode). The best "smart random" sequence is the one with lowest free energy out of all 10,000 random generated sequences, as the representative of random sequences. This sequence actually is the left most plot in the "smart random" cloud

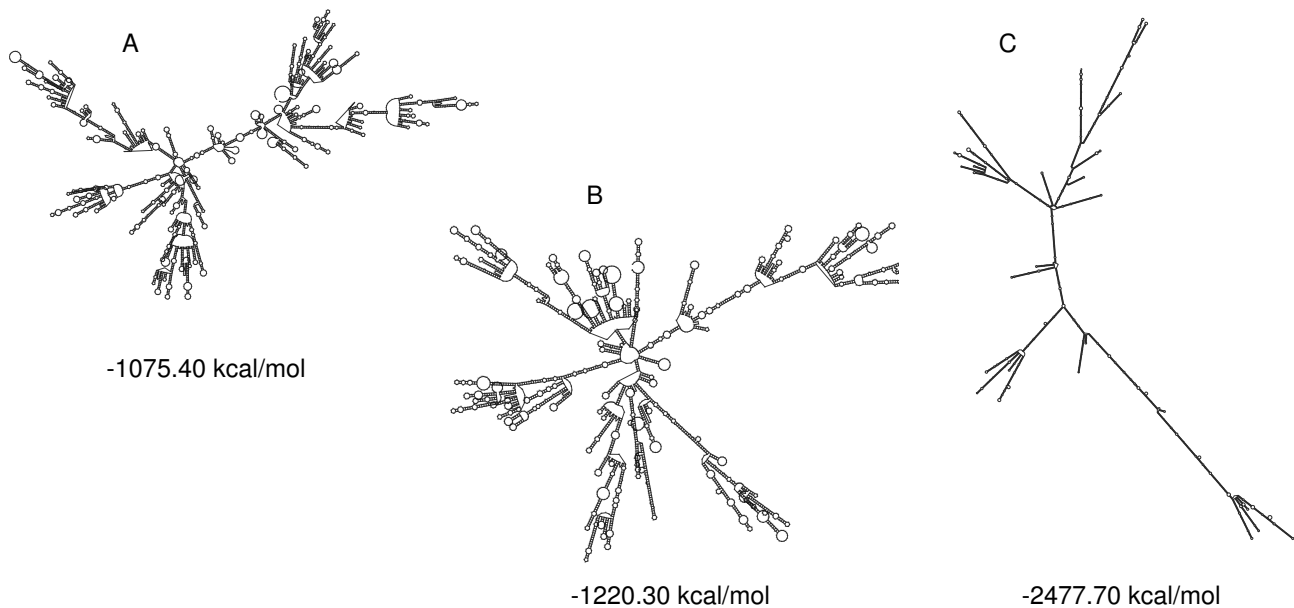


**Fig. 10.** Different mRNA sequences that translate into the spike protein of SARS-CoV-2. **A:** Wildtype sequence. **B:** The best mRNA sequence (with lowest free energy) out of 10,000 random generated sequences. **C:** The best mRNA sequence (with lowest free energy) by LinearDesign.

(orange plots) in Figure 9. The secondary structure of the wildtype sequence is predicted by Vienna RNAfold,<sup>12</sup> while the structures of the random sequences are by LinearFold-V<sup>3</sup> because it is too slow to use RNAfold for all 10,000 sequences with length more than 3,000 *nt*. We can see that the secondary structures of the wildtype and random sequences have lots of loops, and our designed sequence has longer helices and less loops, which makes the structure more stable.

#### 4. Discussion

The mRNA design problem is of utmost importance, especially for mRNA vaccines during the current COVID-19 pandemic. We reduced this problem into a classical problem in formal language theory and computational linguistics, namely the intersection of a CFG (encoding the energy model) with a DFA (encoding the mRNA search space). This reduction provides a natural  $O(n^3)$ -time CKY-style bottom-up algorithm, where  $n$  is the mRNA sequence length, but this algorithm might still be too slow for long proteins such as the spike protein of SARS-CoV-2, a promising candidate for an mRNA vaccine. Inspired by our recent work of LinearFold, we then developed a left-to-right algorithm, LinearDesign, which employs beam search to reduce the runtime to  $O(n)$ , with the cost of exact search. LinearDesign is orders of magnitude faster than exact search (i.e.,  $b = +\infty$ ) and suffers only a small loss in free energy. For example, for this spike protein, LinearDesign can finish in 16 minutes while exact search takes 1.6 hours, and the free energy difference is only 0.6%. We also developed two algorithms for incorporating codon optimality (CAI) into the consideration, one using  $k$ -best algorithms to compute suboptimal sequences and one directly integrating CAI into dynamic programming. Our work provides efficient computational tools to speed up and improve mRNA vaccine development.

**ACKNOWLEDGMENTS.** We thank Rhiju Das for introducing the mRNA design problem to us. D.H.M. is supported by National Institutes of Health grant R01GM076485.

#### References

- David M Mauger, B Joseph Cabral, Vladimir Presnyak, Stephen V Su, David W Reid, Brooke Goodman, Kristian Link, Nikhil Khatwani, John Reynders, Melissa J Moore, et al. mRNA structure regulates protein expression through changes in functional half-life. *Proceedings of the National Academy of Sciences U.S.A.*, 116(48):24075–24083, 2019.
- E. Rivas. The four ingredients of single-sequence RNA secondary structure prediction. a unifying perspective. *RNA Biology*, 10(7):1185–1196, 2013.
- Liang Huang, He Zhang, Dezhong Deng, Kai Zhao, Kaibo Liu, David A Hendrix, and David H Mathews. LinearFold: linear-time approximate RNA folding by 5'-to-3' dynamic programming and beam search. *Bioinformatics*, 35(14):i295–i304, 07 2019.
- Barry Cohen and Steven Skiena. Natural selection and algorithmic design of mRNA. *Journal of Computational Biology*, 10(3-4):419–432, 2003.
- Goro Terai, Satoshi Kamegai, and Kiyoshi Asai. CDSfold: an algorithm for designing a protein-coding sequence with the most stable secondary structure. *Bioinformatics*, 32(6):828–834, 2016.
- John E. Hopcroft, Rajeev Motwani, and Jeffrey D. Ullman. *Introduction to Automata Theory, Languages, and Computation (3rd Edition)*. Addison-Wesley Longman Publishing Co., Inc., USA, 2006.
- Ruth Nussinov and Ann B Jacobson. Fast algorithm for predicting the secondary structure of single-stranded RNA. *Proceedings of the National Academy of Sciences U.S.A.*, 77(11):6309–6313, 1980.
- R. Durbin, S. Eddy, A. Krogh, and G. Mitchison. *Biological Sequence Analysis: Probabilistic Models of Proteins and Nucleic Acids*. Cambridge University Press, Cambridge, UK, 1998.
- Liang Huang, Suphan Fayong, and Yang Guo. Structured perceptron with inexact search. In *Proceedings of the 2012 Conference of the North American Chapter of the Association for Computational Linguistics: Human Language Technologies*, pages 142–151, Montréal, Canada, June 2012. Association for Computational Linguistics.
- David H Mathews, Jeffrey Sabina, Michael Zuker, and Douglas H Turner. Expanded sequence dependence of thermodynamic parameters improves prediction of RNA secondary structure. *Journal of Molecular Biology*, 288(5):911–940, 1999.
- David H. Mathews, Matthew D. Disney, Jessica L. Childs, Susan J. Schroeder, Michael Zuker, and Douglas H. Turner. Incorporating chemical modification constraints into a dynamic programming algorithm for prediction of RNA secondary structure. *Proceedings of the National Academy of Sciences U.S.A.*, 101(19):7287–7292, 2004.
- Ronny Lorenz, Stephan H Bernhart, Christian Hoener Zu Siederdisen, Hakim Tafer, Christoph Flamm, Peter F Stadler, and Ivo L Hofacker. ViennaRNA package 2.0. *Algorithms for Molecular Biology*, 6(1):1, 2011.
- Liang Huang and David Chiang. Better k-best parsing. *Proceedings of the Ninth International Workshop on Parsing Technologies*, pages 53–64, 2005.
- M. Zuker. On finding all suboptimal foldings of an RNA molecule. *Science*, 244(4900):48–52, 1989.
- S. Wuchty, W. Fontana, I. Hofacker, and P. Schuster. Complete suboptimal folding of RNA and the stability of secondary structures. *Biopolymers*, 49(2):145–65, 1999.
- David H Mathews. Revolutions in RNA secondary structure prediction. *Journal of molecular biology*, 359(3):526–532, 2006.
- UniProt Consortium. Uniprot: a hub for protein information. *Nucleic Acids Research*, 42:D204–D12, 2005.
- Paul M Sharp and Wen-Hsiung Li. The codon adaptation index—a measure of directional synonymous codon usage bias, and its potential applications. *Nucleic Acids Research*, 15(3):1281–1295, 1987.

# Supporting Information

## LinearDesign: Efficient Algorithms for Optimized mRNA Sequence Design

He Zhang, Liang Zhang, Ziyu Li, Kaibo Liu, Boxiang Liu, David H. Mathews and Liang Huang

```
1: function UPDATE( $q_i, q_j, score, backpointer$ )
2:   if  $score < best[q_i, q_j]$  then                                     ▷ minimizing weight
3:      $best[q_i, q_j] \leftarrow score$ 
4:      $back[q_i, q_j] \leftarrow backpointer$ 

1: function BACKTRACE( $q_i, q_j$ )
2:    $backpointer \leftarrow back[q_i, q_j]$ 
3:   if  $type(backpointer)$  is string then                               ▷ singleton
4:      $nuc_i \leftarrow backpointer$ 
5:     return  $nuc_i, ". "$ 
6:   if  $length(backpointer) = 4$  then                                     ▷ pairing:  $S \xrightarrow{-1} A S U | \dots$ 
7:      $nuc_i, q_{i+1}, q_{j-1}, nuc_{j-1} \leftarrow backpointer$ 
8:      $seq, struct \leftarrow BACKTRACE(q_{i+1}, q_{j-1})$ 
9:     return  $nuc_i + seq + nuc_{j-1}, "(" + struct + ")"$ 
10:  else                                                                 ▷ bifurcation:  $S \xrightarrow{0} S S$ 
11:     $q_k \leftarrow backpointer$ 
12:     $seq_1, struct_1 \leftarrow BACKTRACE(q_i, q_k)$ 
13:     $seq_2, struct_2 \leftarrow BACKTRACE(q_k, q_j)$ 
14:    return  $seq_1 + seq_2, struct_1 + struct_2$ 

1: function BACKTRACE2( $q_i, q_j$ )
6:   if  $length(backpointer) = 5$  then                                     ▷ pairing:  $S \xrightarrow{-1} S A S U | \dots$ 
7:      $q_{k-1}, nuc_{i-1}, q_k, q_{j-1}, nuc_{j-1} \leftarrow backpointer$ 
8:      $seq_1, struct_1 \leftarrow BACKTRACE2(q_i, q_{k-1})$ 
9:      $seq_2, struct_2 \leftarrow BACKTRACE2(q_k, q_{j-1})$ 
10:    return  $seq_1 + nuc_{i-1} + seq_2 + nuc_{j-1}, struct_1 + "(" + struct_2 + ")"$ 
11:  else                                                                 ▷ unpaired:  $S \xrightarrow{0} S N$ 
12:     $q_{j-1}, nuc_{j-1} \leftarrow backpointer$ 
13:     $seq, struct \leftarrow BACKTRACE2(q_i, q_{j-1})$ 
14:    return  $seq + nuc_{j-1}, struct + ". "$ 

1: function BEAMPRUNE( $Q, j, b$ )
2:    $cands \leftarrow hash()$                                              ▷ hash table: from node  $q_i$  to combined score  $best[q_0, q_i] + best[q_i, q_j]$ 
3:   for each  $q_j \in nodes(j)$  do
4:     for each key  $(q_i, q_j) \in best$  do
5:        $cands[q_i] \leftarrow best[q_0, q_i] + best[q_i, q_j]$          ▷  $best[q_0, q_i]$  as prefix score
6:    $cands \leftarrow SELECTTOPB(cands, b)$                                ▷ select top- $b$  by score
7:   for each key  $(q, q_j) \in best$  do
8:     if key  $q_i$  not in  $cands$  then
9:       delete  $(q_i, q_j)$  in  $best$                                      ▷ prune out low-scoring states
```

**Fig. S11.** The pseudocode for UPDATE, BACKTRACE (used in BOTTOMUPDESIGN), and BACKTRACE2 and BEAMPRUNE (used in LINEARDISIGN) functions.